Nature Environment and Pollution Technology
An International Quarterly Scientific Journal

p-ISSN: 0972-6268
(Print copies up to 2016)
e-ISSN: 2395-3454

Vol. 24 | No. 1 | Article ID D1703 | 2025

Original Research Paper

https://doi.org/10.46488/NEPT.2025.v24i01.D1703

Open Access Journal

Mechanism and Behavior of Phosphorus Adsorption from Water by Biochar Forms Derived from Macadamia Husks

Nguyen Van Phuong†
Institute of Science, Engineering and Environmental Management, Industrial University of Ho Chi Minh City, Vietnam
†Corresponding Author: Nguyen Van Phuong; nguyenvanphuong@iuh.edu.vn

Abbreviation: Nat. Env. & Poll. Technol.
Website: www.neptjournal.com

Received: 25-07-2024
Revised: 23-08-2024
Accepted: 25-08-2024

Key Words:

Biochar
Macadamia husk
Phosphorus adsorption
Langmuir model
Freundlich model
Kinetic model

Citation for the Paper:

Phuong, N. V., 2025. Mechanism and behavior of phosphorus adsorption from water by biochar forms derived from Macadamia husks. *Nature Environment and Pollution Technology*, 24(1), D1703. https://doi.org/10.46488/NEPT.2025.v24i01.D1703

Note: From year 2025, the journal uses Article ID instead of page numbers in citation of the published articles.

Copyright: © 2025 by the authors
Licensee: Technoscience Publications
This article is an open access article distributed under the terms and conditions of the Creative Commons Attribution (CC BY) license (https://creativecommons.org/licenses/by/4.0/).

ABSTRACT

High phosphate content in water causes eutrophication, leading to many risks to the aquatic environment and human health. This study used biochar derived from macadamia husks at the pyrolysis temperatures (300, 450, and 600℃) to remove P from water. Adsorption parameters such as initial pH, biochar dosage, initial P concentration, and adsorption time when biochar was exposed to the P solution were determined. The results show that pH 4 is optimal for P removal with biochar pyrolyzed at 300 and 450°C, while pH 6 gives biochar 600°C, biochar dosage 10 $g.L^{-1}$, concentration Initial P 25-200 $mg.L^{-1}$ and adsorption time 40 minutes for 3 types of biochar. The maximum P adsorption capacity is 20.07, 20.03, and 20.03 $mg.L^{-1}$ corresponding to 3 forms of biochar 300, 450, and 600°C. P adsorption data were consistent with the Freundlich isotherm model for all three biochar forms. The pseudo-second-order kinetic model was suitable for all three types of biochar, showing that the main adsorption mechanism is a surface chemical reaction. The study suggested that hydrogen bonding plays an important role in the adsorption of P onto biochar derived from macadamia husks. This study indicates that biochar derived from macadamia husks pyrolyzed at temperatures of 300, 450, and 600°C are all potentially effective and low-cost adsorbents for phosphate removal from water.

INTRODUCTION

Excess phosphorus (P) released into surface water can lead to eutrophication, disrupting the ecological balance. This can affect human health (Xu et al. 2022). Meanwhile, P is a non-renewable resource, so effectively recovering P will be a solution in the circular economy, which can prevent risks caused by excess P from water (Xu et al. 2022).

Various methods for P removal and recovery from wastewater have been explored, including biological methods, chemical precipitation, electrochemical methods, coagulation, membrane separation, and adsorption (Choi et al. 2019). Biological methods that rely mainly on the metabolism of certain microorganisms are considered promising (Xu et al. 2022). However, this method is only suitable for low P concentrations; the removal rate is usually low (30% to 40%) (Xu et al. 2022) and fluctuates according to operating conditions (Choi et al. 2019). Chemical methods can achieve the purpose of P removal (Xu et al. 2022). However, the cost is high, and the possibility of causing pollution due to sludge generation. Electrochemical processes are limited when wastewater contains many anionic compounds and the need to replace electrodes is often costly (Choi et al. 2019). The adsorption method is not only highly effective, simple to operate, and produces less sludge but can also be applied to treat wastewater with many different concentrations. Therefore, the adsorption method has attracted more and more attention worldwide (Xu et al. 2022).

There are many adsorbent materials, such as bentonite, zeolite, activated carbon, biochar, etc., used (Xu et al. 2022). Recently, the biochar-based adsorption

process has received more attention because of its effective adsorption capacity and low cost (Choi et al. 2019). Furthermore, it is possible to utilize the adsorbed product for agricultural production purposes.

The adsorption properties of biochar depend on the type of raw material, heating rate, pyrolysis temperature, and retention time (Luo et al. 2023). However, the P adsorption capacity of biochar is very different because phosphate anions are often repelled by some negatively charged surfaces of biochar, leading to very different P adsorption levels. Among 22 types of biochar derived from plants regarding the ability to adsorb P–PO_4, only 4 types of biochar were found to show the ability to adsorb P–PO_4 from water (Zhang et al. 2020).

The adsorption mechanism includes several interactions, such as physical adsorption, surface precipitation, complexation, electrostatic attraction, and ion exchange (Luo et al. 2023). SEM and TEM analysis determined the surface area and porosity of biochar; however, there is no correlation between biochar surface area and P adsorption capacity from water (Nobaharan et al. 2021). Therefore, exploring the P adsorption mechanism and behavior of biochar will improve the application efficiency of biochar from water P treatment.

Macadamia is an economically valuable crop that is grown around the world. Macadamia nut production produces a large amount of biomass residue, known as macadamia nut husks (Vu et al. 2023). In Dak Nong, Vietnam with about 1100 hectares, the yield is 1.5 tons of seeds/ha, and waste husks account for 75%. Currently, this waste source is mainly left to decompose naturally, which is highly wasteful. Biochar production is a trend in the circular economy in agriculture.

Therefore, studying the ability to adsorb P from water using biochar derived from macadamia husks pyrolyzed at different temperatures was investigated by determining different operating factors such as water pH, biochar dosage, initial P concentration, adsorption time as well as adsorption behavior and mechanism. The evaluation objective of the experiment is mainly based on P adsorption capacity but also considers the effectiveness of P treatment from water.

MATERIALS AND METHODS

Sampling Methods

The macadamia husk sample was taken in December 2023 from the Macadamia Nut Processing Company, DakNong Province, Vietnam. The husks were pre-dried, crushed to <5 mm, and dried in an oven (Shellab Drying Oven, USA) at 60°C for 24 hours.

Chemicals

Chemicals used in the study were of analytical purity: NaH_2PO_4, $K_2Cr_2O_7$, $SnCl_2$, $(NH_4)_6Mo_7O_{24}.4H_2O$ from Merck. EDTA, KCl, HCl, NH_4Cl, NaOH, HNO_3, NaOH, H_2O_2, H_2SO_4, $NaHCO_3$ from China.

Preparing Biochar

Biochar preparation was simulated according to a previous study (Phuong et al. 2021), in which processed macadamia husks were pyrolyzed in a Naberthem P330 furnace (Germany) at three temperatures: 300, 450, 600ºC (Bio 300, Bio 450, and Bio 600). The heating rate was 10°C.min^{-1}, the heat retention was 2 hours, and it cooled overnight in the furnace. The pyrolysis product was crushed through a 1 mm sieve and stored at 4°C. The biochar samples were then used to determine some of the surface properties of the biochar and used for further experiments.

Some biochar surface properties such as pH, pH_{pzc} (Tu. 2016), and total organic carbon (TOC) (Tan. 2011), P content in water were determined using the photometric method on SPECTROSCOPY, Model: GENESYS 10S UV-VIS, 6-/1-CELL, Brand: Thermo scientific/USA. A spectrophotometer FT/IR-4700 type A in 350-4000 cm^{-1} was used to determine the functional groups of biochar.

Experimental Design to Investigate Factors Affecting the Adsorption of Phosphorus

Initial pH: The experiment was performed in a 60 mL polypropylene tube by mixing 0.3 g of various types of biochar (Bio 300, Bio 450, and Bio 600) with 30 mL of 200 mg.L^{-1} P solution, initial pH values (2, 4, 6, and 8 were adjusted with HCl and NaOH). This mixture was shaken on a GFL 3015 circular shaker (Germany) at 350 rpm for 24 h. The pH was not adjusted during the experiments. The tubes were centrifuged at 4000 rpm for 15 min using a DLAB DM 0636 centrifuge and filtered through a 0.22 µm filter. The P content in the filtered solution was determined. Adsorption experiments were conducted at least three times.

Biochar dosage: The pH selected from the experiments of the initial pH section will be set to continue for experiments investigating biochar dosage (0.0; 0.10; 0.3; 0.5, 0.7; 1, 0 g) along with fixed conditions such as 30 mL of 200 mg.L^{-1} P solution, shaking speed of 350 rpm for 24 h.

Initial P concentration: The pH is selected from the experiments of the initial pH section, and the biochar dosage from the biochar dosage section will be set to continue for the experiments investigating the initial P concentration (0; 17, 25, 50, 100, 150 and 200 mg.L^{-1}) along with fixed conditions such as shaking speed of 350 rpm for 24 h.

Adsorption time: The pH is selected from the experiments of the initial pH section, and the biochar dosage from the biochar dosage section will be set to continue for the experiments to investigate the effect of adsorption time with the following conditions as P content of 200 mg.L^{-1}, and shaking speed of 350 rpm. Periodic patterns 20, 40, 80, and 160 minutes were removed (enough time to achieve equilibrium according to preliminary experiments). Analyze the P solution after filtration.

Evaluation of the adsorption behavior and mechanism includes evaluation of adsorption kinetics based on pseudo-first- and second-order kinetic models and equilibrium evaluation based on Langmuir and Freundlich adsorption models.

Data Analysis

Calculation

Adsorption capacity, mg/g: $q_i = \frac{(C_0 - C_i).V}{m}$ ...(1)

In which:

C_0 (mg.L^{-1}): initial concentration of P

C_i (mg.L^{-1}): P concentration of sample i in solution at equilibrium time

V (L): volume of P solution

m (g): mass of biochar sample

q_i (mg.g^{-1}): P adsorption capacity of sample i at equilibrium time.

K_L is the Langmuir adsorption constant (L.mg^{-1}).

Langmuir isotherm equation:

$$\frac{1}{q_i} = \frac{1}{K_L q_0}\frac{1}{C_i} + \frac{1}{q_0} \quad ...(2)$$

Freundlich isotherm equation:Hay:

$$q = y/m = K_F C^{\frac{1}{n_F}} \quad ...(3)$$

Hay:

$$Logq_i = \frac{1}{n_F} logC_i + logK_F \quad ...(4)$$

In which:

n_F: Freundlich isotherm constant, expressing P adsorption intensity.

K_F: Freundlich adsorption isotherm constant, expressing adsorption capacity.

Pseudo-first-order kinetic equation:

$$Ln(q_e - q_t) - Lnq_e = -k_1 t \quad ...(5)$$

or $$Ln(q_e - q_t) = -k_1 t + Lnq_e \quad ...(6)$$

Pseudo-second-order kinetic equation:

$$\frac{1}{q_t} = \frac{1}{t}\frac{1}{k_2 q_e^2} + \frac{1}{q_e} \quad ...(7)$$

Where:

q_e: P adsorption capacity at equilibrium (mg g^{-1})

q_t: P the adsorption capacity at time t (mg g^{-1})

k_1 (1 min^{-1}): constants of pseudo-first-order and pseudo-second-order kinetic

và k_2 (g mg^{-1} min^{-1}): constants of pseudo-first-order and pseudo-second-order kinetic

t (min): time adsorption.

Data Processing

Data was collected, calculated, and graphed based on software available in Excel 2016. Oneway ANOVA analysis on SPSS 23.

RESULTS AND DISCUSSION

Some Surface Properties of Biochar

Surface properties of biochar derived from Macadamia husk pyrolyzed at different temperatures include recovery efficiency (%H), pH, pHpzc, number of H^+ groups, cation exchange capacity (CEC), available phosphorus and ammonium nitrogen were determined and are presented in detail in Table 1. Biochar recovery efficiency (%H) in the study was 49.1; 32.0; 27.2% corresponds to pyrolysis temperatures of 300, 450 and 600°C. The results show that as the pyrolysis temperature increases, the biochar recovery efficiency decreases. This is explained by increasing the pyrolysis temperature, and the loss of volatile organic substances increases (Lehmann & Joseph 2015). Similar results were also found in the study by Li et al. (2024), with a recovery efficiency of 34.5% when pyrolysis of cotton (Gossypium sp. L.) straw at 500°C (Li et al. 2024). The results of analyzing the average recovery efficiency values of biochar samples ($p<0.05$) on SPSS 23 were statistically significant differences. This shows that each type of organic matter in the macadamia husk has been decomposed according to thermal fraction. Specifically, at the pyrolysis temperature of 300°C, only hemicellulose decomposes (220–315°C); at 450°C, cellulose decomposes, and at 600°C, lignin decomposes mainly (Huang et al. 2022).

The biochar pH value increased to 7.09, 8.06, and 8.04, respectively, for biochar samples Bio 300, Bio 450, and Bio 600. The difference in pH value in samples Bio 300 and Bio 450 is significantly different. This can explain why the hemicellulose in the macadamia husks component was well decomposed at a temperature of 300°C (Huang et al. 2022).

Table 1: Recovery efficiency and some surface chemical properties of biochar.

t ℃	% H	pH	pHpzc	%TOC
300	49.1[c]	7.09[a]	6.35[a]	41[b]
SD	0.3	0.11	0.14	2
450	32.0[b]	8.06[b]	7.87[b]	29[a]
SD	0.2	0.01	0.01	2
600	27.2[a]	8.04[b]	7.96[c]	30[a]
SD	0.1	0.06	0.11	2

A,b, and c in the same column indicate significant differences ($p<0.05$); SD: standard deviation; H%: biochar recovery efficiency; pHpzc: pH at the point of zero charges.

The pH values of Bio 450 and Bio 600 samples did not change significantly, possibly due to the decomposition of organic substances from 450 to 600 °C occurring at the same time as the formation of shorter-chain organic compounds (Huang et al. 2022).

The pHpzc value increased by 6.35, 6.87, and 7.96, respectively, with Bio 300, Bio 450, and Bio 600; the difference in pH values is statistically significant. The obtained results were smaller than those of biochar from coffee husks, according to previous research (Phuong et al. 2021). This can be explained by the difference in lignocellulosic material composition, which is common for materials containing lignocellulose.

TOC content tends to decrease with increasing pyrolysis temperature, Table 1. Specifically, TOC is 41, 29, and 30%, corresponding to pyrolysis temperatures of 300, 450, and 600°C. The research results were 26, 20, and 1% higher than materials from coffee husks (Phuong et al. 2021). This shows that the material origin affects the TOC content in biochar. One-way ANOVA analysis showed that TOC content changes in biochar M450 and M600 were not significant, which may explain the slow destruction of organic matter such as lignin.

FTIR spectrum shows that the peaks at 3435 cm^{-1} belonging to –OH vibration, 1603 cm^{-1} for C=C, and C=O in the aromatic ring, and 1693 cm^{-1} for C=O in carboxyl group (Feng et al. 2021, Xiong et al. 2024). The strong, broad FTIR spectrum at wavelength 3414 cm^{-1} is mainly responsible for the stretching vibration of the hydroxyl group OH– (alcohol and phenolic). This shows that the –OH, –COOH groups can participate in electron exchange reactions (hydrogen bond formation) during the adsorption process (Xiong et al. 2024). The absorption peak ranges from 1600 to 1500 cm^{-1}, indicating the existence of an extended aromatic C=C ring. Therefore, the peak at 1603 cm^{-1} is considered to be the relaxation of the aromatic C=C ring. This intensity gradually decreases at the pyrolysis temperature of 450°C and is completely lost at 600°C. The research results are similar to Angın & Şensöz's research, which shows that aromatic rings disappear when the pyrolysis temperature increases (Angın & Şensöz 2014). At 1024 cm^{-1}, the sharp peak with moderate intensity illustrates the C–O–C stretching of ester groups in cellulose and hemicellulose (Kenchannavar & Surenjan 2022, Tomczyk et al. 2020). These peaks will also decrease or disappear with increasing pyrolysis temperature (Angın & Şensöz 2014). Fig. 1 shows that the peaks of the hydroxyl group and carbonyl group shift to 3030 cm^{-1} and decrease sharply in intensity when increasing the pyrolysis temperature. The decrease in the intensity of the bands described above shows that the acidic functional groups of the surface have decreased with increasing pyrolysis temperature (Angın & Şensöz 2014). The reduction or

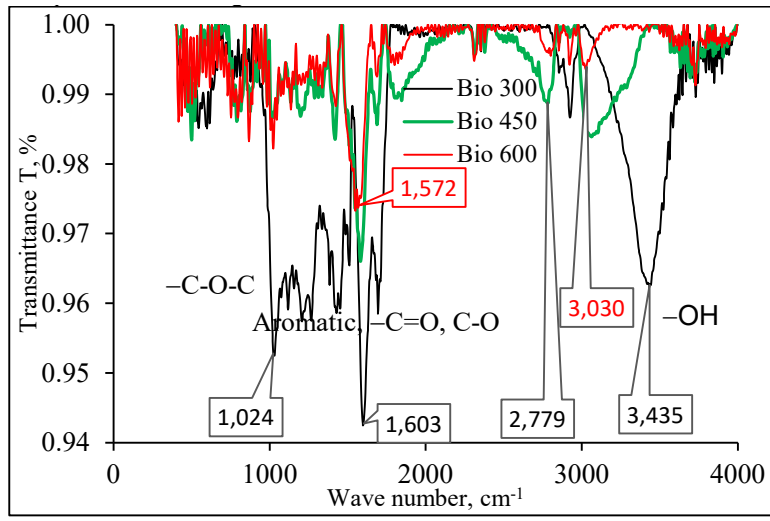

Fig. 1: FT-IR spectra of biochar forms.

disappearance of these peaks is related to the degradation and depolymerization of cellulose, hemicellulose, and lignin (Huang et al. 2022).

This can be explained by the fact that the pyrolysis of organic materials in the temperature range of 350–650°C cracked and formed new chemical bonds in the biomass, thereby forming new functional groups such as carboxyl, phenol, ether... (Tomczyk et al. 2020). These functional groups can form hydrogen bonds, greatly increasing the adsorption process of substances capable of forming hydrogen bonds or acting as electron donors or acceptors.

Factors Affecting the Adsorption of P from Water onto Biochar

Initial solution pH: The results of investigating the initial pH effect on the P adsorption capacity of biochar derived from macadamia nut husks prepared at different pyrolysis temperatures are presented in Fig. 2. For 300˚C biochar, Fig. 2a shows that the adsorption capacity increased slightly from 18.44 to 18.45 mg g^{-1} when the initial pH was 2 and 4. As the initial pH increased to 6, the adsorption capacity decreased sharply to 16.7 mg g^{-1}, the decrease was statistically significant and maintained an insignificant change of 16.5 and 17.15 mg g^{-1} when the initial pH was 6 and 8 respectively.

Similarly, in the case of Bio 450, Fig. 2b shows that the adsorption capacity increased from 14.5 to 18.6 mg g^{-1}, this increase was significant when the initial pH of the solution increased from 2 to 4. Then, when increasing to pH 6, the adsorption capacity decreased significantly to 16.9 $mg.g^{-1}$. When the initial pH increased to 8, 10, the capacity increased again and maintained at 17.7 $mg.g^{-1}$.

For Bio 600, the adsorption capacity increased from 16.4 to 16.9 and 17.6 $mg.g^{-1}$ when the initial pH of the solution was 2, 4, and 6, respectively. This increase is statistically significant. Then, when the initial pH increased to 8, the adsorption capacity decreased to 16.4 $mg.g^{-1}$, a significant decrease and negligible change at pH 10 (16.8 $mg.g^{-1}$), Fig. 2c.

This can be explained because, at different initial pH values, P can exist in different forms. Specifically, at pH 2, P exists mainly in the form of H_3PO_4 (pKa1= 2.12), so the P adsorption capacity at this pH is low. At pH 4-7, P exists mainly in the form of $H_2PO_4^-$ (pKa2=7.2) and will adsorb to the biochar surface through electrostatic bonds. Because the pHpzc of the three forms of biochar all have values > 6.3, when the solution pH is < 6.3, the positively charged biochar surface will create favorable conditions for adsorbing phosphorus anions based on the force of electrostatic bonding (Luo et al. 2023). At pH > 8, this pH value is higher than the pHpzc of all three forms of biochar, then the biochar surface is negatively charged. The adsorption capacity of P anions decreases due to electrostatic repulsion (Nobaharan et al. 2021). Furthermore, as pH increases, OH^- ions also increase, leading to competition for P anion adsorption sites on the biochar surface (Luo et al. 2023).

In the case of Bio 300, at pH 2, the P adsorption capacity is still higher than Bio 450 or Bio 600. This can be explained by the more diverse organic properties of Bio 300, such as containing lipids and cellulose, which causes it to dissociate less (Tomczyk et al. 2020).

When considering the P removal efficiency of biochar samples, Fig. 2d shows that at pH 4, the highest treatment efficiency is 92.8, 93.2, and 84.7%, corresponding to Bio 300, Bio 450, and Bio 600. Therefore, the study chose pH 4 for the next experiments when using Bio 300 and Bio 450, choosing pH 6 for Bio 600.

Biochar dosage: The results of investigating the effects of biochar dosage prepared at 300˚C are presented in Fig. 3a. The results showed that the adsorption capacity decreased sharply when increasing the biochar content in the solution; the adsorption capacity decreased from 38.7 to 17.2; 7.6, and 5.4 $mg.g^{-1}$ corresponds to biochar contents of 3, 10, 17, and 23 $g.L^{-1}$. This level decreased with statistical significance. While at dosages of 23 and 33 $g.L^{-1}$, the adsorption capacity did not change significantly.

With Bio 450°C presented in Fig. 3b, it shows that the adsorption capacity decreased by 41.8, 19.1, 10.4, 7.4, and 4.6 $mg.g^{-1}$ corresponding to biochar dosages of 3, 10, 17, 23, and 33 $g.L^{-1}$. The reduction was significant at biochar dosages of 3, 10, 23 $g.L^{-1}$. Between 23 and 33 $g.L^{-1}$, the change in adsorption capacity was not statistically significant.

With Bio 600, the research results are presented in Fig. 3c. The results showed that the P adsorption capacity decreased by 41.2, 15.3, and 8.7 $mg.g^{-1}$, corresponding to biochar dosages of 3, 10, and 17 $g.L^{-1}$. This sequential decrease is statistically significant. P adsorption capacity at biochar dosages of 23 and 33 $g.L^{-1}$ was not statistically significant.

Overall, the results of the study can be explained as increasing the adsorbent dosage leading to increased active sites and binding sites for phosphate ions on the surface of the biochar. This creates favorable conditions for phosphorus adsorption. However, the P removal efficiency does not increase and is stable when the adsorbent dosage is greater than 10 $g.L^{-1}$. This is explained by the fact that all experiments were conducted at the same initial P concentration (200 $mg.L^{-1}$). This condition is thought to be caused by the aggregation of biochar particles, reducing the

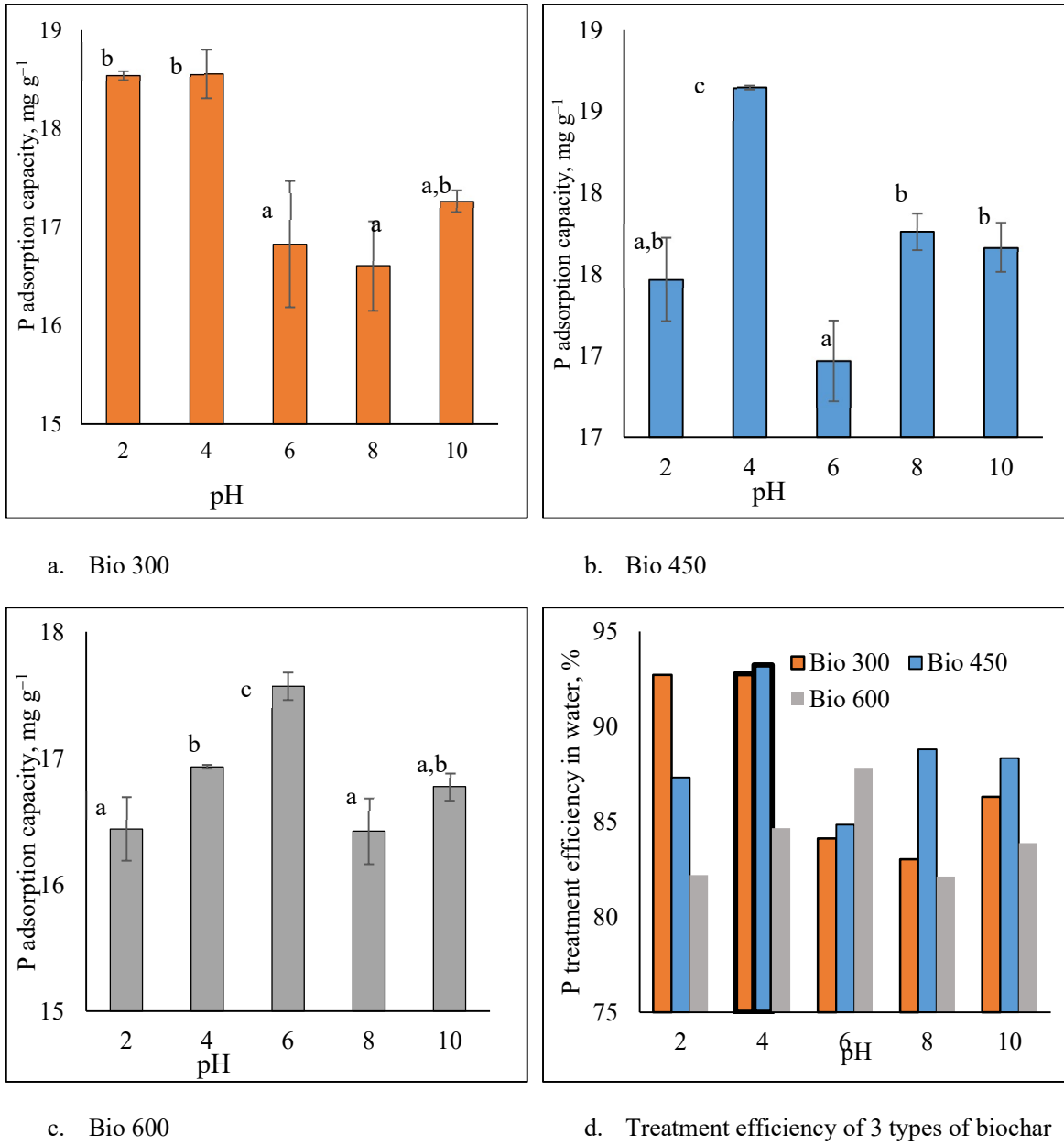

a. Bio 300 b. Bio 450

c. Bio 600 d. Treatment efficiency of 3 types of biochar

Fig. 2: Effect of pH on P adsorption capacity (mg.g^{-1}) of biochar at different pyrolysis temperatures. Different letters represent significant differences.

available surface area and leading to reduced P adsorption capacity (Luo et al. 2022).

The optimal dosage of biochar needs to be determined depending on the user's purpose. If the goal is to remove phosphate from wastewater, then more biochar is needed to remove it. If phosphorus adsorption with biochar is used as a fertilizer or to save costs, less biochar should be chosen. In this study, the adsorption capacity is based on consideration of treatment efficiency.

Experimental results showed that at pH 4, the P content is 200 mg.L^{-1}, so the biochar dosage should be 10 mg.L^{-1}. These parameters are used for further experiments.

Initial P concentrations: The results of investigating the effect of initial P concentrations (C_0) on the adsorption capacity of Bio 300 are presented in Fig. 4a. The results show that as C_0 increases, the adsorption capacity q also increases. Specifically, the P adsorption capacity increased by 0, 2.45; 4.84, 9.75, 14.19, and 18.56 mg.g^{-1}, corresponding to C_0

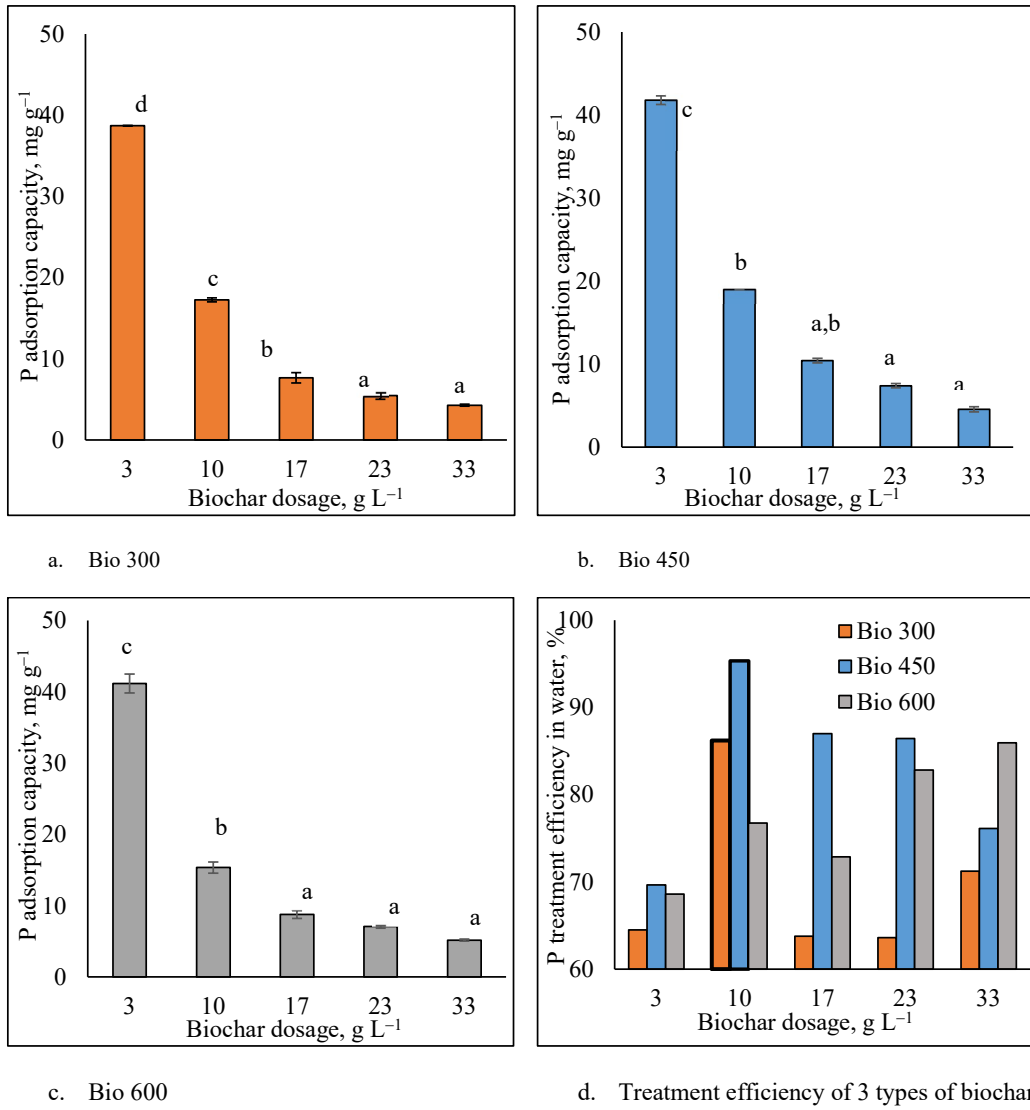

a. Bio 300 b. Bio 450

c. Bio 600 d. Treatment efficiency of 3 types of biochar

Fig. 3: Effect of biochar dosage and P adsorption capacity (mg g^{-1}) of biochar samples. Different letters represent significant differences.

concentrations of 0, 25, 50, 100, 150, and 200 mg.P.L^{-1}, respectively. The results of Oneway ANOVA analysis on SPSS 23 show that all values of P adsorption capacity are statistically significantly different. Research results show that the adsorption process continues under the current experimental conditions.

In the case of Bio 450, Fig. 4b, the research results show that the adsorption capacity increased from 0.00, 2.39, 4.83; 9.77, 14.48, and 18.65 mg.g^{-1} correspond to the initial C_0 values as in the Bio 300 experiment. Research results also show that the increase process is statistically significantly different in C_0 values in the experiment. The research results also show signs of saturated adsorption under current experimental conditions.

Similarly, for Bio 600, Fig. 4c shows that the adsorption capacity increases corresponding to the increase in initial concentration C_0. The adsorption capacity values increased significantly with the surveyed C_0 values. Specifically, the adsorption capacity increased by 0.00, 2.19, 4.03, 8.23, 13.03, and 17.66 mg.g^{-1} correspond to C_0 values of 0, 25, 50, 100, 150, and 200 mg L^{-1}, respectively. There was no sign of adsorption saturation under the experimental conditions.

Evaluation results of P treatment efficiency from water when conducting experiments under conditions such as pH 4 (or 6), biochar dosage 10 g.L^{-1}, and initial P content in the range of 25 to 200 mg.L^{-1} showed that P removal efficiency decreased with increasing pyrolysis temperature.

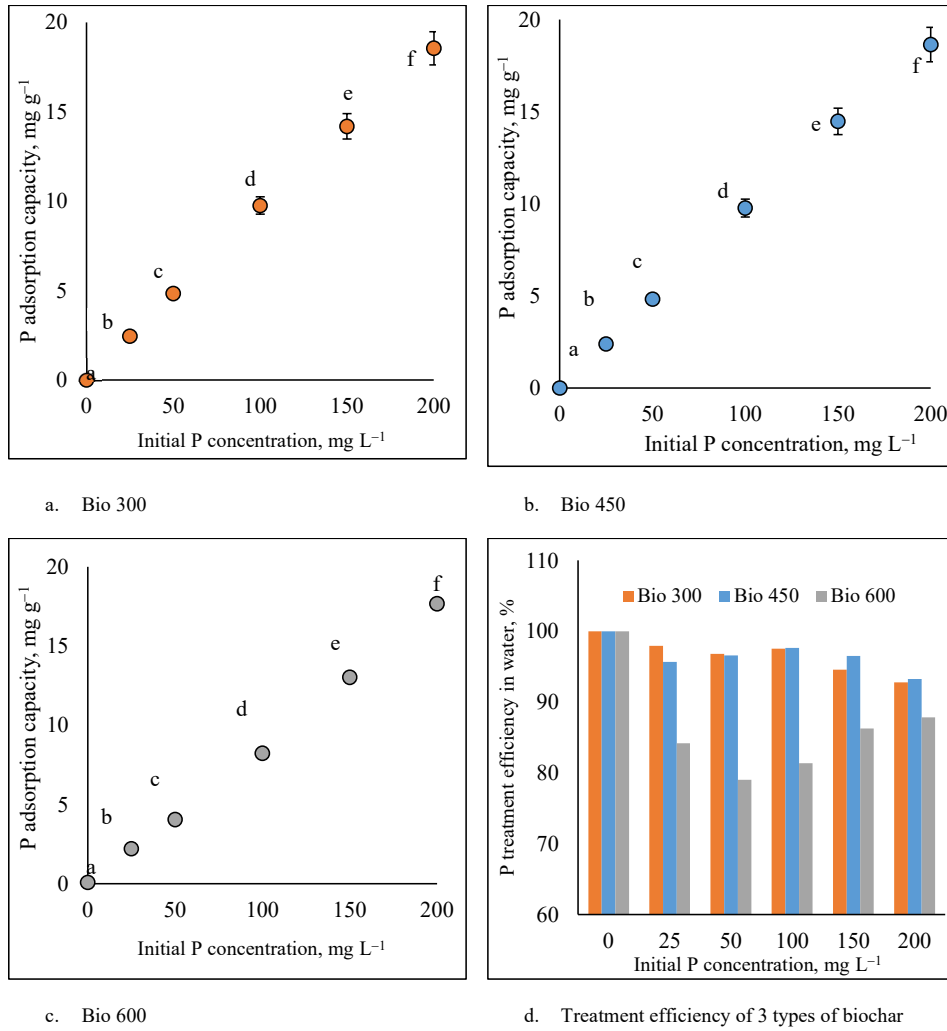

a. Bio 300 b. Bio 450

c. Bio 600 d. Treatment efficiency of 3 types of biochar

Fig. 4: Effect of initial P concentration and P adsorption capacity (mg g^{-1}) of biochar samples. Different letters represent significant differences.

Specifically, P treatment efficiency (%) fluctuated (98.0-92.8); (95.7-93.2); (84.2-87.8) corresponding to the Bio 300, Bio 450, and Bio 600 samples, respectively, Fig. 4c. This result is much larger than the results reported by Nobaharan et al. that peanut hull-derived biochar had a P removal efficiency of 61% at an initial P concentration of 5 mg.L^{-1} at pH 7, as well as with magnesium-modified corn biochar that only achieved a P removal efficiency of 90% at an initial P concentration of 84 mg.L^{-1}, pH 7.8 (Nobaharan et al. 2021).

The results show that the adsorption process has not reached the adsorption saturation state under experimental conditions. This can be explained in the form of an adsorption curve of this type, also known as a constant partition isotherm (Tan 2011). The adsorption process is characterized by a continuous distribution of the solute in the solution and the adsorbent. This type of adsorption is common when new adsorption sites appear as soon as the solute is adsorbed from the solution (Tan 2011). Then, the newly formed hydrogen bonds continue to develop through the bridge P P–OH... O=P. This bond is stronger than the hydrogen bond of water (MacLeod & Rosei 2011).

Adsorption time: Investigation of the time factor on the P adsorption capacity of Bio 300 is presented in Fig. 5a. The results showed that the adsorption capacity increased rapidly at 19.98 mg.g^{-1} in 20 minutes. After that, the adsorption capacity continued to increase slightly from 20.04 to 20.06 mg.g^{-1} at 40 and 80 minutes, and the process increased insignificantly after 160 minutes, at which time it was considered to stop. This result is similar in Bio 450 and Bio 600 (Fig. 4b and Fig. 4c). Specifically, with Bio 450, after 20 min, the adsorption capacity was 19.92 mg.g^{-1}. After 40

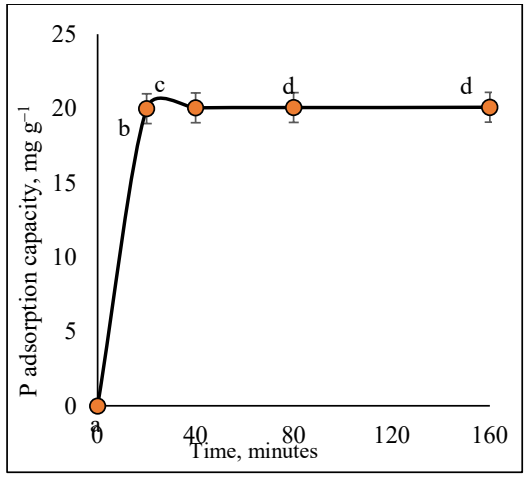

a. Bio 300

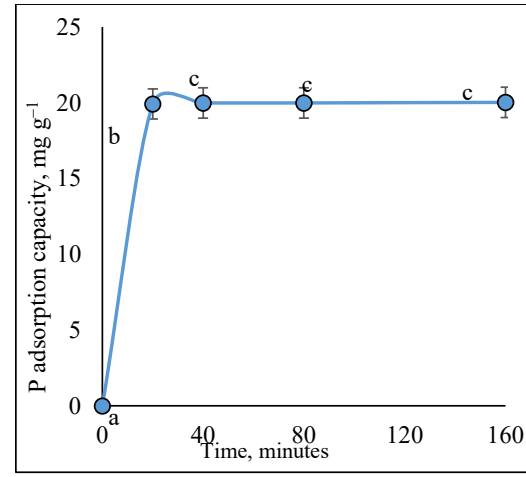

b. Bio 450

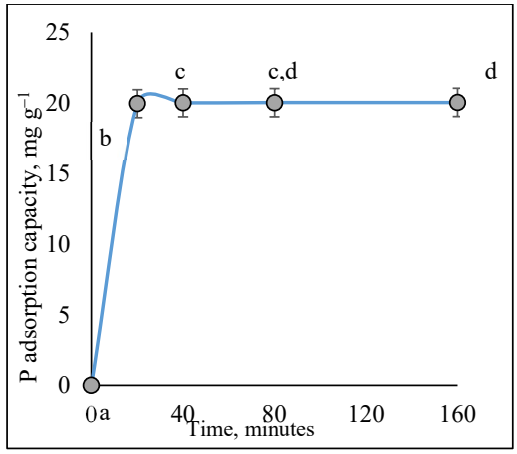

c. Bio 600

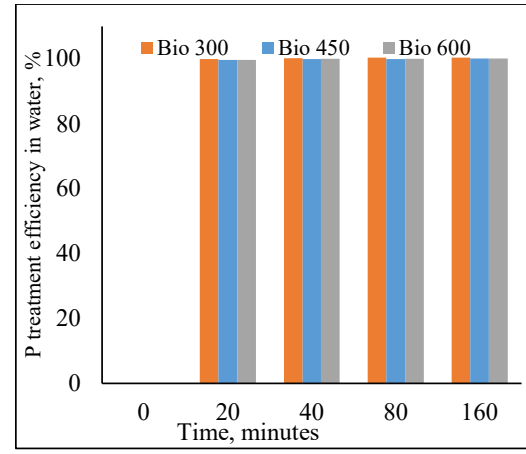

d. Treatment efficiency of 3 types of biochar

Fig. 5: Effect of time on P adsorption capacity (mg g^{-1}) of biochar samples. Different letters represent significant differences.

minutes, it was 19.98 mg $g^{-1,}$ and it was considered to stop. With Bio 600, it is 19.94 and 20.00 mg g^{-1}.

Results from kinetic studies of P adsorption have shown that there are two stages in the P adsorption process on biochar. The chemical adsorption phase occurred rapidly and was followed by a surface diffusion control phase when the surface adsorption sites were saturated. (Nobaharan et al. 2021).

Experimental results showed that the time to reach the saturated adsorption state occurred in about 20 to 40 minutes for all 3 forms of biochar.

Adsorption Equilibrium

Further data modeling according to the Langmuir model shows that only Bio 300 is more suitable than other forms of biochar due to the large correlation coefficient R^2 (0.97) and the calculated maximum adsorption capacity value (q_0=19, 59 mg g^{-1}) is close to the experimental value (18.6 mg.g^{-1}), Table 2. The research results were higher than biochar derived from pine trees at a maximum of 13,898 mg g^{-1}; maize-straw is 8.809 mg g^{-1} (Zhao et al. 2017). This result shows that the phosphate adsorption process is monolayer adsorption (Feng et al. 2021). Meanwhile, the results of calculating q_0 and the experimental results of both Bio 450 and Bio 600 samples were very different, so the Langmuir model was not appropriate. Besides, when considering the Freundlich model, the 3 types of biochar were all suitable because R^2 was > 0.92. K_F were 4.06; 2.61; 0.41; and 1/n_F is 0.61; 1.15; 1.10. The value $1/n_F$ was a function of the adsorption intensity during the adsorption process, and it represents heterogeneity (Feng et al. 2021)

Table 2: P adsorption equilibrium parameters.

Models	Pyrolysis temperature	Parameters		R^2	q(ex)
		q_0 [mg.g^{-1}]	K_L		
Langmuir	300°C	19.6	0.28	0.97	18.6
	450°C	-36.3	-0.06	0.91	18.6
	600°C	73.43	0.01	0.95	17.7
Freundlich		$\mathbf{1/n_F}$	$\mathbf{K_F}$		
	300°C	0.61	4.06	0.95	
	450°C	1.15	2.61	0.93	
	600°C	1.10	0.41	0.92	

q(ex): P adsorption capacity in the experiment

This finding indicates that during the P adsorption process of three types of biochar with multilayer layers, many heterogeneous surfaces appeared on the biochar surface, and the adsorption may be related to the interactions of chemical interaction between the adsorbent and adsorbent. An explanation of the research results was also found in Yi and Chen (2018).

P Adsorption Kinetics

Calculated data of kinetic parameters showed that the pseudo-second-order kinetic model (Table 3) is more suitable, with a correlation coefficient $R^2 > 0.97$ and the calculated adsorption capacity value (qe). Compared with the experimental adsorption value (qex), it is almost the same. Specifically, qe calculated from the second-order kinetic equation is 20.09, 20.03, and 20.04 mg.g^{-1}, very close to the experimental value (qex) for three types of biochar, Bio 300, Bio 450, and Bio 600, respectively, which are 20.07, 20.03 and 20.03 mg.g^{-1} (Table 3). Therefore, the P adsorption rate of the three types of biochar is controlled by the chemical adsorption mechanism, consistent with previous reports (Feng et al. 2021). Then, the kinetics of P adsorption is mainly due to chemical bonding or chemisorption involving electron sharing between phosphate ion species and biochar (Feng et al. 2021). The adsorption rate of the three types of biochar fluctuated insignificantly in the range of 0.444-0.525.

Table 3: Calculation results of kinetic parameters.

Models	Pyrolysis temperature	qe [mg.g^{-1}]	Kinetic constant	qex	R^2
Pseudo-first-order kinetic	300°C	0.10	k_1=0.009	20.07	0.74
	450°C	0.17	k_1=0.005	20.03	0.85
	600°C	0.09	k_1=0.011	20.03	0.87
Pseudo-second-order kinetic	300°C	20.09	k_2=0.491	20.07	0.98
	450°C	20.03	k_2=0.444	20.03	0.97
	600°C	20.04	k_2 =0.525	20.03	0.98

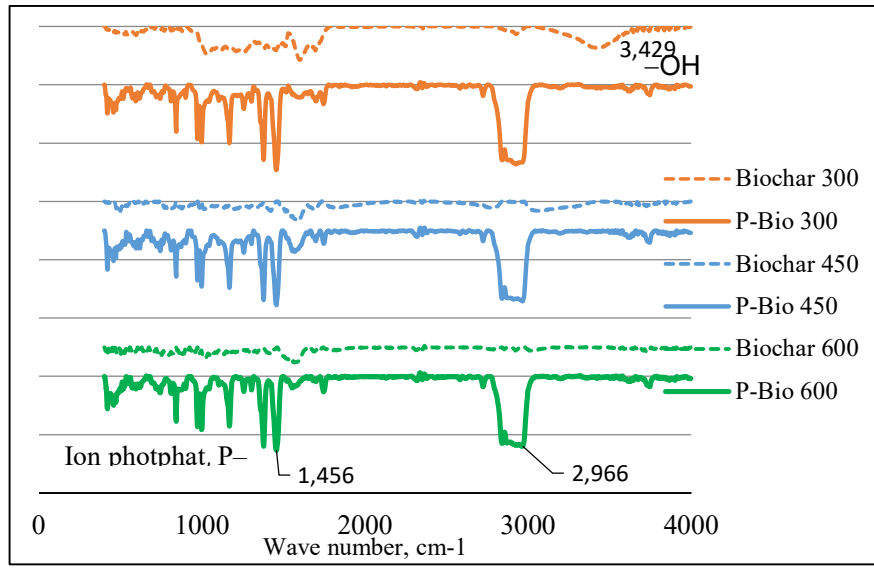

Fig. 6: FT-IR spectra of biochar samples before adsorption (Bio 300, Bio 450, and Bio 600) and after P adsorption (P-Bio 300; P-Bio 450 and P-Bio 600).

Fig. 6 shows the appearance of peaks of O–H groups of hydrogen bonds shifted to 2932 $cm^{-1,}$ and this shows that biochar functional groups may have a role in the P adsorption process through the bridging. hydrogen P–OH...O=P (MacLeod & Rosei 2011). From FTIR spectrum analysis, the increase in peak intensity and shift of the spectrum peak showed that the adsorption may be due to interactions arising after adsorption. Meanwhile, functional groups OH and aromatic carbon can also play an important role in the P adsorption process (Kenchannavar & Surenjan 2022). Asymmetric P–O vibrations of the adsorbed $H_2PO_4^-$ and HPO_4^{2-} groups were also detected in the range of 900-1454 cm^{-1} and appeared in all 3 biochar samples after adsorption (MacLeod & Rosei 2011). The research findings have a basis for confirming that hydrogen bonding plays an important role in the adsorption process of phosphorus ions on the surface of biochar derived from macadamia husks.

Overall, the results of the study confirmed the potential of using biochar derived from macadamia shells (a locally available agricultural waste) at pyrolysis temperatures to remove (adsorb) P from water. The product of the adsorption process can not only be used as a soil conditioner (improving pH, providing organic carbon) but also as a fertilizer (providing P). The contribution of this solution to the circular economy in agriculture (using waste) is well-founded.

CONCLUSIONS

Biochar derived from macadamia husks was pyrolyzed at 300, 450, and 600. Characteristics of biochar forms were determined. The results showed that factors such as initial pH, biochar dosage, initial P concentration, and adsorption time affected the P adsorption capacity of three types of biochar. Besides, the phosphate adsorption capacity at pyrolysis temperatures of 300 and 450°C is higher than biochar pyrolysis at 600°C. Freundlich isotherm and pseudo-second-order kinetic models were found to be most suitable for phosphate adsorption onto biochar forms. This shows that chemisorption interactions occur on the biochar surface through the hydrogen bond bridge P=O...HO–P. Research has shown that biochar produced from macadamia husks can adsorb P from water and that biochar pyrolysis temperature has a non-significant impact on the adsorption capacity of biochar. The study was only conducted in the laboratory under controlled conditions. Therefore, when implemented in practice, additional studies are needed, such as adsorption in the presence of ions (such as ammonium, nitrate, and sulfate), and the particle size of the biochar should also be considered, then the potential risks can be assessed more accurately.

ACKNOWLEDGMENTS

Thank you to students of course 15, Institute of Science, Engineering and Environmental Management, for your support. We thank the reviewers for their comments to improve the quality of the manuscript.

REFERENCES

Angın, D. and Şensöz, S., 2014. Effect of pyrolysis temperature on chemical and surface properties of biochar of rapeseed (*Brassica napus* L.). *International Journal of Phytoremediation,* 16(7-8), pp.684-693.

Choi, Y.K., Jang, H.M., Kan, E., Wallace, A.R. and Sun, W., 2019. Adsorption of phosphate in water on a novel calcium hydroxide-coated dairy manure-derived biochar. *Environmental Engineering Research,* 24(3), pp.434-442.

Feng, Y., Zhao, D., Qiu, S., He, Q., Luo, Y., Zhang, K., Shen, S. and Wang, F., 2021. Adsorption of phosphate in aqueous phase by biochar prepared from sheep manure and modified by oyster shells. *ACS Omega,* 6(48), pp.33046-33056.

Huang, X., Ren, J., Ran, J.-Y., Qin, C.L., Yang, Z.Q. and Cao, J.P., 2022. Recent advances in pyrolysis of cellulose to value-added chemicals. *Fuel Processing Technology,* 229, p.107175.

Kenchannavar, P. and Surenjan, A., 2022. Application of circular economy in wastewater treatment using biochar-based adsorbent derived from sewage sludge. *IOP Conference Series: Earth and Environmental Science,* 142, p.101242.

Lehmann, J. and Joseph, S., 2015. *Biochar for Environmental Management: Science, Technology and Implementation*. Routledge.

Li, Y., Zhao, B., Wang, L., Li, Y., Wang, T., Jia, Y. and Zhao, M., 2024. Competitive adsorption of Cd (II) and Zn (II) on biochar, loess, and biochar-loess mixture. *Nature Environment & Pollution Technology,* 23(1), p.65.

Luo, D., Wang, L., Nan, H., Cao, Y., Wang, H., Kumar, T.V. and Wang, C., 2022. Phosphorus adsorption by functionalized biochar: a review. *Environmental Chemistry Letters,* 7, pp.1-29.

Luo, D., Wang, L., Nan, H., Cao, Y., Wang, H., Kumar, T.V. and Wang, C., 2023. Phosphorus adsorption by functionalized biochar: a review. *Environmental Chemistry Letters,* 21(1), pp.497-524.

MacLeod, J. and Rosei, F., 2011. 3.02-Directed assembly of nanostructures. In: D.L. Andrews, G.D. Scholes and G.P. Wiederrecht, eds. *Comprehensive Nanoscience and Technology*. Academic Press.

Nobaharan, K., Bagheri Novair, S., Asgari Lajayer, B. and van Hullebusch, E.D., 2021. Phosphorus removal from wastewater: the potential use of biochar and the key controlling factors. *Water,* 13(4), p.517.

Phuong, N.V., Hoang, N.K., Luan, L.V. and Tan, L., 2021. Evaluation of NH_4^+ adsorption capacity in water of coffee husk-derived biochar at different pyrolysis temperatures. *International Journal of Agronomy,* 21, pp.1-9.

Tan, K.H., 2011. *Principles of Soil Chemistry*. Taylor and Francis Group, LLC.

Tomczyk, A., Sokołowska, Z. and Boguta, P., 2020. Biochar physicochemical properties: pyrolysis temperature and feedstock kind effects. *Reviews in Environmental Science and Bio/Technology,* 19(1), pp.191-215.

Tu, T., 2016. Physical and chemical characterization of biochar derived from rice husk. *Hue University Journal of Science,* 120, pp.233-247.

Vu, N.L., Nguyen, N.D., Tran-Nguyen, P.L., Nguyen, H.V., Dinh, T.M.T. and Nguyen, H.N., 2023. Evolution of properties of macadamia husk throughout gasification: hints for a zero-waste energy production system. *Biomass and Bioenergy,* 171, p.106735.

Xiong, M., Dai, G., Sun, R. and Zhao, Z., 2024. Passivation effect of corn vinasse biochar on heavy metal lead in paddy soil of Pb-Zn mining area. *Nature Environment & Pollution Technology,* 23(1).

Xu, Y., Liao, H., Zhang, J., Lu, H., He, X., Zhang, Y., Wu, Z., Wang, H. and Lu, M., 2022. A novel Ca-modified biochar for efficient recovery of phosphorus from aqueous solution and its application as a phosphorus biofertilizer. *Nanomaterials,* 12(16), p.2755.

Yi, M. and Chen, Y., 2018. Enhanced phosphate adsorption on Ca-Mg-loaded biochar derived from tobacco stems. *Water Science and Technology,* 78(11), pp.2427-2436.

Zhang, M., Song, G., Gelardi, D.L., Huang, L., Khan, E., Mašek, O., Parikh, S.J. and Ok, Y.S., 2020. Evaluating biochar and its modifications for the removal of ammonium, nitrate, and phosphate in water. *Water Research,* 186, p.116303.

Zhao, S., Wang, B., Gao, Q., Gao, Y. and Liu, S., 2017. Adsorption of phosphorus by different biochars. *Spectroscopy Letters,* 50(2), pp.73-80.